arXiv:physics/0504182v1 [physics.chem-ph] 26 Apr 2005

Plasmon-mediated Polarization Anomalies in Surface Enhanced Raman Scattering (SERS)

E. C. Le Ru* and P. G. Etchegoin†

The McDiarmid Institute for Advanced Materials and Nanotechnology
School of Chemical and Physical Sciences
Victoria University of Wellington
PO Box 600, Wellington, New Zealand

(Dated: February 2, 2008)

We discuss the effect of the local field polarization in metallic nanostructures where large field enhancements can be induced by excitation of localized surface plasmons. To demonstrate the importance of these effects, we study a few model systems in 2D and 3D. As an experimental probe of this effect, we suggest to use depolarization ratios in Surface Enhanced Raman Spectroscopy (SERS) measurements. We attempt to relate the polarization of the local field to the depolarization ratios in SERS conditions. This approach could also lead to some better understanding of the SERS mechanisms at a microscopic level.

PACS numbers: 78.67.-n, 78.20.Bh, 78.67.Bf, 73.20.Mf

I. INTRODUCTION

Raman depolarization ratios of molecular vibrations are one of the most fundamental properties of inelastic light scattering in liquids[1]; they are widely used in conjunction with other types of spectroscopies to infer indirectly the symmetry of molecular vibrational modes. Essentially, every vibration in a molecule can be assigned to a given irreducible representation (or linear combinations of them) of either the overall symmetry point group of the molecule or one of its sub-structures. Once the symmetry is known the Raman tensor of the vibration with respect to a fixed molecular coordinates system is also known. A collection of randomly oriented molecules will produce average intensities for parallel ($I_\parallel$) or perpendicularly ($I_\perp$) polarized scattering configurations in Raman spectroscopy, from where a well defined depolarization ratio $\rho \equiv I_\perp/I_\parallel$ follows. Both ($I_\parallel$) and ($I_\perp$) only depend on tensor invariants which do not change under rotations of the reference frame. This is a canonical textbook problem in non-resonant inelastic light scattering of liquids and poly-crystalline solids[1], which has also its exact counterpart in elastic (Rayleigh) scattering (with the linear polarizability tensor playing the role of the Raman tensor)[2]. There is ample theoretical and experimental understanding of this effect in Raman scattering, which started with the pioneering work of Porto, Skinner, and Nielsen[3, 4] in the 60's in the angular dependence of inelastic light scattering of simple liquids.

Notwithstanding, under Surface Enhanced Raman Scattering (SERS) conditions in liquids (colloids) depolarization ratios of Raman signals of the analyte molecules (typically dyes) are most of the time anomalous and, in addition, show some laser wavelength dependence. It is interesting to understand the origin of these anomalies for such a fundamental physical property of the scattering process like the depolarization ratio. The problem is intimately related to the issue of *local fields* in SERS and in plasmon-supporting structures in general. SERS is made possible by highly localized plasmon resonance excitations called hot-spots, which achieve large optical amplifications and boost Raman scattering signals by several orders of magnitude[5, 6]. Highly (subwavelength) localized hot-spots have been proposed and studied both theoretically[7, 8] and experimentally[9, 10, 11]. It is the purpose of this paper to shed some light on the polarization aspects of hot-spots and how they affect basic properties of the symmetry of the scattering. We also explore how these effects could be used in principle to learn more about the nature of hot-spots, local fields, and laser-field amplifications by plasmons.

We would like to address in the paper two main issues:

- Local-field polarization effects are often overlooked in most treatments of the SERS effect, but should be important for many essential properties of the scattering process. We shall show that depolarization ratios are mainly determined by plasmons in a SERS environment. The most striking demonstration of this effect is the breakdown of normal depolarization ratios in single isolated objects, as demonstrated in the next sections.

- Depolarization ratios can, in principle, assert something about the SERS enhancement mechanism itself and, in addition, the equally important issue of molecular orientation and geometry of the analyte on the metallic surface.

All these issues will be addressed with a variety of examples for different geometries and assumptions, together with some experimental evidence for anomalous depolarization ratios at the end.

*Electronic address: Eric.LeRu@vuw.ac.nz
†Electronic address: Pablo.Etchegoin@vuw.ac.nz

II. BASIC DEFINITIONS

SERS enhancements by one or several objects depend on the geometry of the objects themselves, their symmetry, and their orientation in space with respect to the fixed scattering polarization directions in the laboratory frame. In addition, the scattering can come from a single analyte (molecule) in a specific place on the surface of the metal, or from the multiple contributions of a distribution of molecules in many places. Last, but not least, the Raman tensor of the analyte can be of many different types (symmetries); hence the orientation of the main axes of the tensor with respect to the metal surface at specific points has to be specified also. In effect, the possibilities are endless. We need to start by imposing some restrictions on the type of objects, Raman tensors, and molecular orientations at the surface that we will examine.

We first address the issue of the origin of the SERS signal in terms of single/multiple dyes contributions. Interpretations of the data based on single molecule detection have been claimed many times in the past[15, 16, 17]. If single molecule detection is achievable then the polarization properties of the local field at the position of the molecule will be the only parameter that counts. The same situation happens if the presence of analyte is widespread over the metal but there are high intensity hot-spots dominating the signal. In such a situation, the polarization properties of a specific place in space and/or the orientation of the Raman tensor of one or a few molecules are the main factors determining the symmetry of the scattering event. The polarization properties would then be an average (over time or space) of many of these hot-spots. Polarization studies in SERS in single molecule limits are very rare[18, 19] and not fully understood in our opinion.

The most common experimental situation, however, is one in which there are many contributions from many analytes which are spatially distributed in different places and, accordingly, are exposed to different local fields. This is for example the case of colloidal solutions of gold or silver particles at relatively high ($\sim$ 100 nM) concentration of analyte and measured in immersion. If conditions are chosen so that the solution is stable, we can rule out the presence of large clusters of particles (which would precipitate) and the signal must therefore come from single particles or possibly pairs of particles (either stable pairs or dynamical pairs formed during close encounters of two particles). In order to observe a good SERS signal from such solutions, higher analyte concentrations are required, corresponding typically to $\sim 10^2$-10^4 molecules per particle. To study the polarization effects in such systems, one has to consider the signals of all these molecules and also average over all possible orientations of the particles. This is only possible in simple cases and it is the main reason for the restrictions we shall impose in the modelling.

A. Basic geometries and Raman tensors

We shall discuss here a few model cases: spherical particles, elliptical particles, and dimers (two particles in close proximity). In each case, we will model the SERS depolarization ratio, which can be measured experimentally, under different assumptions.

There are three main factors that can affect the calculated depolarization ratio ρ.

- The Raman tensor of the probe molecules: We will consider the cases of an isotropic Raman tensor (Iso) and of a uniaxial tensor. These are two extreme cases of a variety of molecular symmetries present in real analytes. Many common SERS analytes (like rhodamine 6G) have strongly uniaxial Raman tensors for most of their vibrations.

- The adsorption configuration of the molecule: This is obviously an important factor when the Raman tensor is not isotropic. For the uniaxial case, we therefore need a further assumption about the way the molecule adsorbs on the metal surface and, in particular, how the main axis is oriented with respect to the surface. We will consider the two extreme cases of a molecule adsorbed with its axis tangential (Tan) or normal ($Norm$) to the surface. We will also consider the case where the adsorption geometry is random ($Rand$). In this latter case, all possible orientations of the molecules are considered and averaged.

- Finally, the way the molecule couples to the local field polarization: This is also a very important aspect because it is directly related to the SERS enhancements mechanism and has in our opinion been overlooked.

We shall have a small digression on this latter issue here. If we consider a molecule with a highly uniaxial Raman tensor oriented along $\vec{e}_m$, then the excited dipole has the form (case A):

$$\vec{p}^A = \alpha \left(\vec{E} \cdot \vec{e}_m \right) \vec{e}_m, \tag{1}$$

where $\vec{E}$ is the local electric field and α is the main component of the uniaxial polarizability. This is a case often found in normal Raman scattering. The intensity scattered and detected in the far field in a given direction $\vec{e}_d$, along a given polarization $\vec{e}_p$ ($\vec{e}_p \perp \vec{e}_d$) is then $I \propto |\vec{p} \cdot \vec{e}_p|^2$. However, if we use this expression in SERS conditions, the SERS signal is only proportional to the power of two of the local field enhancement factor (and not power of four as usually assumed[5]). In order to obtain a power of four in the scattering efficiency, we need to model the enhancement process due to re-emission of this dipole. One could use the following expression (case

B):

$$\vec{p}^{B} = \frac{\alpha|\vec{E}|}{|\vec{E}_0|}\left(\vec{E}\cdot\vec{e}_m\right)\vec{e}_m. \quad (2)$$

Anywise, this implies that the enhancement in re-emission has no polarization dependence. Another view is to assume that the excited dipole couples only to the local field enhancement along its direction; we then get (case C):

$$\vec{p}^{C} = \frac{\alpha}{|\vec{E}_0|}\left(\vec{E}\cdot\vec{e}_m\right)^2\vec{e}_m. \quad (3)$$

In both cases, we have also assumed that the local field enhancements relevant to re-emission were the same as those derived for excitation. This is a common assumption but is not necessarily valid. Assuming we know the local field enhancements for a given geometry, we can then calculate the polarization property of the SERS signal for each of the cases A, B, and C at each point of the surface S of our metallic structure/s. These can then be integrated over the surface, assuming a continuous distribution of probe molecules of type Iso, Tan, $Norm$, or $Rand$.

B. Symmetries and averages

As an example, and to provide a basis for further discussion, we carried out calculations for simple model systems in 2 dimensions (2D). The structures are in the plane (yOz) and the exciting beam is coming from the perpendicular direction (Ox), with a field polarization along z. The local fields at the surface are calculated within the electrostatics approximation. The calculations were carried out numerically using finite element modelling described elsewhere[20]. We assume that the signal is detected in the far field along (Ox) and analyzed for parallel (Oz) and perpendicular (Oy) polarizations. For a given structure, we calculated $I_\parallel$ and $I_\perp$ for each of our assumptions. $\vec{n}$ ($\vec{t}$) denotes the unit normal (tangential) vector at any point on the metallic surface. We therefore used the following expressions:

$$I_\parallel^{Iso-A} = \int_S |E_z|^2\, dS, \quad (4)$$

$$I_\parallel^{Iso-B} = I_\parallel^{Iso-C} = \int_S \left|\vec{E}\right|^2 |E_z|^2\, dS, \quad (5)$$

$$I_\parallel^{Norm-A} = \int_S \left|\vec{E}\cdot\vec{n}\right|^2 n_z^2 dS, \quad (6)$$

$$I_\parallel^{Norm-B} = \int_S \left|\vec{E}\right|^2 \left|\vec{E}\cdot\vec{n}\right|^2 n_z^2 dS, \quad (7)$$

and

$$I_\parallel^{Norm-C} = \int_S \left|\vec{E}\cdot\vec{n}\right|^4 n_z^2 dS. \quad (8)$$

Similar expressions for $Tan-A, -B, -C$ replacing $\vec{n}$ with $\vec{t}$ are also obtained. Expressions for $I_\perp$ are obtained by replacing z subscripts with y. We will also for each case estimate the total SERS intensity by means of:

$$I_{Tot} = I_\parallel + I_\perp. \quad (9)$$

For structures without rotational symmetry, the calculations were repeated for 50 different orientations, parameterized by an angle β. The total signals are then obtained by summing over all possible orientations. In our structures, we need only to consider β from 0 to $\pi/2$ by symmetry, so we have:

$$I_\parallel = \int_0^{\pi/2} I_\parallel(\beta) d\beta, \quad (10)$$

and the depolarization ratios is then calculated according to

$$\rho = \frac{I_\perp}{I_\parallel}. \quad (11)$$

In most simulations of metallic structures presented in the literature, such as for ellipses or dimers, only one or two possible orientations are considered. In liquids, contributions from all orientations are averaged and the resulting intensity profile can be very different to that of a single configuration. Independent of polarization effects, we believe that the orientation-averaged SERS intensity profiles presented here provides a new insight into plasmon resonances in liquids.

For the $Rand$ cases, one has to consider all possible molecular orientations. In 2D we restrict ourselves to:

$$\vec{e}_m = \cos(\gamma)\vec{e}_y + \sin(\gamma)\vec{e}_z. \quad (12)$$

Estimating the intensities and averaging over γ, one finds that the results $Rand-B$ and $Rand-C$ can be directly obtained from that of $Iso-B$ (also equal to $Iso-C$), namely:

$$\rho^{Rand-B} = \frac{3\rho^{Iso-B}+1}{\rho^{Iso-B}+3}, \quad (13)$$

$$I_{Tot}^{Rand-B} = \frac{1}{2} I_{Tot}^{Iso-B}, \quad (14)$$

$$\rho^{Rand-C} = \frac{5\rho^{Iso-B}+1}{\rho^{Iso-B}+5}, \quad (15)$$

and

$$I_{Tot}^{Rand-C} = \frac{3}{8} I_{Tot}^{Iso-B}. \quad (16)$$

As a reminder, in non-SERS conditions in 2 dimensions, ρ should be 0 for an isotropic molecule and 1/3 for the uniaxial case (*Rand*).

For all calculations, we used the bulk dielectric constant of Ag (a typical metal for SERS applications) as reproduced by a Drude model with the best fit to tabulated data in the region of interest[21], namely:

$$\epsilon(\lambda) = \epsilon_\infty - \frac{1}{\lambda_p^2 \left(\frac{1}{\lambda^2} + \frac{i}{\Gamma\lambda}\right)}, \tag{17}$$

where $\epsilon_\infty = 4$, $\lambda_p = 141$ nm, $\Gamma = 17000$ nm, and λ is the wavelength. The surrounding medium is water with $\epsilon_m = 1.77$.

III. THE SIMPLEST CASE: SERS BY A SINGLE SYMMETRIC OBJECT

A simple object like a disk in 2D or a sphere in 3D has a well defined main plasmon resonance. If the size of the object (a) is much smaller than the wavelength ($a \ll \lambda$) of the light, then the electrostatic approximation is valid and the resonance occurs at the frequency where $\mathrm{Re}(\epsilon(\lambda)) \approx -\epsilon_m$, or $-2\epsilon_m$ for a disk in 2D or a sphere in 3D, respectively. If ($a \sim \lambda$) on the contrary, retardation effects and higher order multipoles play an increasing role and define additional resonances. The current understanding of the SERS effect is that it benefits from red-shifted plasmon resonances[12] which are either shape/size-related or, more often than not, coming from plasmon-plasmon interactions among particles[13, 14]. These latter resonances are believed to be the dominant contribution to the SERS signal in general.

The case of a 2D sphere (or disk) of radius a, is particularly easy because of the rotational symmetry (no need for different β's in the averaging). It can also be easily solved analytically in the electrostatic approximation. We consider an Ag-disk with complex dielectric function $\epsilon(\lambda)$ in water ($\epsilon_m = 1.77$). The important parameter in such problem is the relative dielectric constant $\epsilon_r = \epsilon/\epsilon_m$. For an incident field $\vec{E}_0 = 1\vec{e}_z$, the local field at a point on the surface with coordinates a, θ is simply the superposition of the incident field and of an induced dipolar field:

$$E_y(\theta) = k\sin(2\theta), \tag{18}$$

$$E_z(\theta) = 1 - k\cos(2\theta), \tag{19}$$

with

$$k = \frac{\epsilon_r - 1}{\epsilon_r + 1}. \tag{20}$$

We can therefore derive the following analytical expressions:

$$\rho^{Iso-A} = \frac{|k|^2/2}{1 + |k|^2/2}, \tag{21}$$

$$\rho^{Iso-B} = \frac{|k|^4/2 + |k|^2/2}{1 + |k|^4/2 + 3|k|^2/2 + 2\mathrm{Re}(k)^2}, \tag{22}$$

$$\rho^{Norm-A} = \rho^{Tan-A} = 1/3, \tag{23}$$

$$\rho^{Norm-C} = \rho^{Tan-C} = 1/5, \tag{24}$$

$$\rho^{Norm-B} = \frac{|\epsilon_r|^2 + 1}{5|\epsilon_r|^2 + 1}, \tag{25}$$

and

$$\rho^{Tan-B} = \frac{|\epsilon_r|^2 + 1}{|\epsilon_r|^2 + 5}, \tag{26}$$

where ρ^{Rand-B} and ρ^{Rand-C} can also be evaluated analytically from the expression of ρ^{Iso-B} using Eqs. (13) and (15).

Figure 1 shows the wavelength dependence of the depolarization ratio under the various assumptions considered here. An important aspect to help distinguish these cases is also the total SERS intensity, which is not reflected in the values of ρ. We know that the SERS signal is usually strong enough to be detected, and any valid assumption should therefore predict a reasonably strong SERS signal in addition to a correct depolarization ratio. We show in Fig. 1 the calculated SERS intensity as a function of wavelength. As can be expected, the three cases where the SERS enhancement is only proportional to the square of the field amplitude (cases A) show a relatively small SERS intensity. These three cases will therefore not be studied any further. All the other cases show a strong enhancement at the localized surface plasmon resonance of the object ($\mathrm{Re}(\epsilon) = -\epsilon_m$, $\lambda \sim 339$ nm in this case). For $Tan-B$ and $Tan-C$, this enhancement drops sharply beyond this resonance, while a small enhancement still exists in the other cases.

This is a very interesting case for more than one reason. It is interesting to see how a large variety of cases is observed for ρ in an object which is arguably one of the simplest SERS enhancing object we can think of. In some cases, $\rho = 1/3$ and is independent of wavelength ($Norm-A$, $Tan-A$) or 1/5 ($Norm-C$, $Tan-C$). In other cases, it increases to 1 close to the surface plasmon resonance and decreases slowly beyond that, towards a limiting value of 1/5 ($Iso-B$), 5/13 ($Rand-C$), or 1/2 ($Rand-B$). $Tan-B$ and $Norm-B$ show a somewhat different behavior, the first showing an increase towards 1, while the latter peaks sharply at 1 before the surface plasmon resonance.

Conceptually, it is interesting to see that for the case of an isotropic probe (which should exhibit $\rho = 0$ in free space) ρ can be as large as 1 as a result of the interaction with the metallic disk ($Iso-B$ at resonance). This is surprising because the disk itself is also isotropic, but *the anisotropy is introduced by excitation of non-isotropic dipolar plasmon resonances in the object.*

This demonstrates clearly that the localized plasmon resonances are crucial in the polarization mechanisms and cannot be excluded from the discussion. It is even clear from Fig. 1 that the plasmon resonances, and not the probe molecules, are the dominant factor in the origin of the depolarization ratios; what counts is *the symmetry of the plasmon resonance for the polarization properties of the scattering.* This summarizes in many ways one of the most important points of this paper.

It is interesting to see, in addition, the reasons for the influence of plasmon resonances in terms of field patterns for the simplest possible case treated in this section. In a way, all the other effects are further degrees of sophistication of this simple example. Figure 2 shows for this 2D case the intensity patterns on the surface for an incident polarization along z of $|E_z|^2$, $|E_y|^2$, and the total field $\left|\vec{E}\right|^2$, at three different wavelengths chosen to be below, at, and above the main surface plasmon resonance of the object ($\lambda = 339$ nm). The case can be solved analytically and all the patterns can be interpreted as a direct superposition of the external field and an equivalent induced dipole on the disk. It is the complex polarizability of the metal that makes the dipole response non-trivial because of the relative amplitude and phase shift of the response with respect to the exciting field. From Fig. 2 we can see that *even if we had molecules with an isotropic Raman tensor (emitting in the same direction as the excitation), the depolarization ratio will be changing with wavelength.* Ignoring the Stokes shift, the integrated intensity on the surface for $|E_y|^2$ divided by that for $|E_z|^2$ will give the depolarization ratio at that wavelength. It is easy to infer by visual inspection that the depolarization ratio will be small at $\lambda = 312$ nm, large at resonance ($\lambda = 339$ nm), and small again at longer wavelengths ($\lambda = 364$ nm). It is large (close to 1) at resonance because the induced dipolar response completely dominates the signal. The (analytical) example in Fig. 2 is possibly the simplest example of plasmons affecting the Raman depolarization ratio by changing the nature of the coupling between the laser and the molecules through the local field. In practise the Raman tensor of the molecule itself will play a role, adding an additional degree of complexity to the problem.

As we shall show later for a particular analyte with a uniaxial Raman tensor, SERS experiments on colloidal solutions show that the depolarization ratio indeed changes with wavelength and ranges from 0.4 to 0.7 in our measurements. This observation therefore rules out some of the cases studied here. We can identify three cases which are compatible with this observation and predict a reasonable SERS intensity: $Iso-B$, $Rand-B$, and $Rand-C$. In order to determine which of these cases is the most realistic, one first needs to look at more realistic models. It is in particular important to determine the effect on ρ of different particle shapes and to assess the validity of using a 2D model to infer 3D properties. Finally retardation effects (not taken into account in the electrostatics approximation) can have some influence on the plasmon resonances and therefore also on ρ. We address some of these issues in the next sections.

IV. SHAPE EFFECTS

To understand at least qualitatively the effects of shape, we will consider the case of an ellipse with an aspect ratio between long and short axes of 1.5. Because we now loose the rotational symmetry, we consider the contributions to the SERS signal from ellipses with 50 possible orientations. Figure 3 shows the calculated total SERS intensity under different assumptions. As expected, the plasmon resonance is now split into two resonances: one red-shifted at 363 nm, the other blue-shifted at 320 nm. In many instances in the literature, excitations along one or the other principal axis are usually considered separately and only one resonance is observed at a time. Both resonances are observed here because all possible orientations are considered and summed. Figure 3 also shows the predicted depolarization ratios. Again, a wide variety of different behaviors are observed, but we will concentrate on the three cases identified previously: $Iso-B$, $Rand-B$, and $Rand-C$. All three show a similar pattern with ρ peaking for $\lambda = 340$ nm to a value at $0.8-0.9$, then at $\lambda = 388$ nm to a value of $0.6-0.8$, and then decreasing to the same limiting value as that observed for the disk.

It is interesting to note that the peaks of ρ do not correlate exactly with the plasmon resonances observed in the SERS intensity. The first peak remains at the plasmon resonance of a sphere, while the second appears at even longer wavelength than the red-shifted plasmon resonance. Also, the maximum value of ρ is now slightly smaller than 1. This can have some important consequences for colloidal solutions with a distribution of sizes and shapes. For a given excitation wavelength λ_L, the SERS signal should have a larger contribution from particles in resonance with this wavelength. If there are many such particles, the depolarization ratio will be determined by these and will then correspond to the dip in Fig. 3 at 363 nm (i.e. ρ is smaller than its maximum value). However, if λ_L is longer than most particle resonances, the measured ρ should correspond to values to the right of the dip in Fig. 3. This could lead to an increase in ρ if λ_L remains close to most resonances, or to a decrease at much longer wavelength. Such considerations are important when interpreting experimental results in colloidal solutions because polydiversity is inevitable.

V. CASE OF A 3D SPHERE

It could be argued that conclusions gained from 2D models on depolarization ratios should be taken with care; it is necessary to estimate the changes that will arise from looking at real 3D cases to gain some insight

on how reliable the qualitative predictions of 2D models are. Numerical simulations in 3D are much more computationally demanding than the 2D cases. To assess the importance of the corrections arising from a full 3D model, we will therefore study the case of a 3D sphere and compare qualitatively the results to the 2D case. Similar to the 2D disk, the 3D sphere problem can be solved analytically in the electrostatics approximation. For an incident field $\vec{E}_0 = 1\vec{e}_z$, the local field outside the sphere is simply the superposition of the incident field and of an induced dipolar field:

$$\vec{E} = 3\kappa\cos(\theta)\vec{e}_r + (1-\kappa)\vec{e}_z, \tag{27}$$

where (r, θ, ϕ) are the standard spherical coordinates and

$$\kappa = \frac{\epsilon_r - 1}{\epsilon_r + 2}. \tag{28}$$

Calculations can be carried out in a similar way as for the 2D case. To illustrate this, we describe below the $Norm-C$, $Tan-C$, and $Iso-B$ cases.

In the $Norm-C$ case, the molecules are assumed to be adsorbed with their main axis normal to the metal surface. The parallel and perpendicular intensities are therefore given by:

$$I_{\parallel}^{Norm-C} = \int_S |\vec{E}\cdot\vec{n}|^4(\vec{n}\cdot\vec{e}_z)^2 dS = \frac{2}{7}\left|1+2\kappa\right|^4, \tag{29}$$

and

$$I_{\perp}^{Norm-C} = \int_S |\vec{E}\cdot\vec{n}|^4(\vec{n}\cdot\vec{e}_y)^2 dS = \frac{2}{35}\left|1+2\kappa\right|^4. \tag{30}$$

The depolarization ratio is then independent of wavelength and equal to $\rho^{Norm-C} = 1/5$, which is the same result as that obtained in 2D.

For the case of $Tan-C$, we assume the molecule is adsorbed with its axis tangential to the metallic surface. However, in 3D, this does not define completely the orientation of the axis, and we therefore need to average over all possible orientations of the molecular axis (tangential to the surface). For this, we assume the axis to be along the unit vector:

$$\vec{e}_m = \cos\gamma\vec{e}_\theta + \sin\gamma\vec{e}_\phi. \tag{31}$$

We then calculate:

$$\begin{aligned} I_{\parallel}^{Tan-C}(\gamma) &= \int_S |\vec{E}\cdot\vec{e}_m|^4(\vec{e}_m\cdot\vec{e}_z)^2 dS & (32)\\ &= \frac{32}{35}\cos^6\gamma\left|1-\kappa\right|^4, & (33)\end{aligned}$$

and

$$\begin{aligned} I_{\perp}^{Tan-C}(\gamma) &= \int_S |\vec{E}\cdot\vec{e}_m|^4(\vec{e}_m\cdot\vec{e}_y)^2 dS & (34)\\ &= \frac{8}{105}\left|1-\kappa\right|^4\cos^4\gamma(1+6\sin^2\gamma). & (35)\end{aligned}$$

Averaging over γ ($0 \le \gamma \le 2\pi$), we obtain:

$$I_{\parallel}^{Tan-C} = \frac{2}{7}\left|1-\kappa\right|^4, \tag{36}$$

and

$$I_{\perp}^{Tan-C} = \frac{2}{35}\left|1-\kappa\right|^4. \tag{37}$$

The depolarization ratio is therefore again $\rho^{Tan-C} = 1/5$, independent of wavelength and equal to the 2D case.

In the 2D section, we identified the cases $Iso-B$, $Rand-B$, and $Rand-C$ as the most interesting. The $Iso-B$ case can be calculated analytically, to wit:

$$\begin{aligned} I_{\parallel}^{Iso-B} &= \frac{2}{105}|1-\kappa|^4 & (38)\\ &\quad \left[(3|\epsilon_r|^2+4)(5|\epsilon_r|^2-2+4\mathrm{Re}(\epsilon_r))+56\right], \end{aligned}$$

and

$$I_{\perp}^{Iso-B} = \frac{6}{35}|1-\kappa|^2|\kappa|^2(3|\epsilon_r|^2+4). \tag{39}$$

Hence, the ratio:

$$\rho^{Iso-B} = \frac{|\epsilon_r-1|^2(3|\epsilon_r|^2+4)}{(3|\epsilon_r|^2+4)(5|\epsilon_r|^2-2+4\mathrm{Re}(\epsilon_r))+56}. \tag{40}$$

For the $Rand-B$ and $Rand-C$ cases, one needs to consider molecules with a random orientation of their axis:

$$\vec{e}_m = \sin\gamma\cos\delta\vec{e}_x + \sin\gamma\sin\delta\vec{e}_y + \cos\gamma\vec{e}_z, \tag{41}$$

with $0 < \gamma < \pi$ and $0 < \delta < 2\pi$. Averaging over these parameters, one can show that:

$$\rho^{Rand-B} = \frac{1+4\rho^{Iso-B}}{3+2\rho^{Iso-B}}, \tag{42}$$

$$I_{Tot}^{Rand-B} = \frac{12}{15}I_{\perp}^{Iso-B} + \frac{8}{15}I_{\parallel}^{Iso-B}, \tag{43}$$

$$\rho^{Rand-C} = \frac{1+6\rho^{Iso-B}}{5+2\rho^{Iso-B}}, \tag{44}$$

and

$$I_{Tot}^{Rand-C} = \frac{12}{35}I_{\perp}^{Iso-B} + \frac{16}{15}I_{\parallel}^{Iso-B}. \tag{45}$$

These results are plotted in Fig. 4, with the equivalent 2D results for comparison. We first notice, as expected, that the resonance profile of the SERS intensity is further red-shifted in the 3D case, peaking at 388 nm ($\mathrm{Re}(\epsilon_r) = -2$) instead of 339 nm ($\mathrm{Re}(\epsilon_r) = -1$). Regarding the depolarization ratios, they show the same qualitative behavior as in 2D with some small quantitative changes: they are smaller for the 3D case below the plasmon resonance, and slightly larger beyond this

resonance tending towards the same value at long wavelength. Also, the maximum depolarization ratio is no longer 1 as in the 2D case but around 0.7-0.9 depending on the case. Finally, the maximum of ρ now occurs slightly before the resonance at around 368 nm. For the cases $Rand-B$ and $Rand-C$, ρ remains quite high, at least larger than 0.5 beyond the resonance, while it goes down to around 0.3 for $Iso-B$.

The overall conclusion of translating the simulation from 2D to 3D shapes is that the essential qualitative features are already contained in the 2D simulation. The quantitative picture will, of course, be different. But the core qualitative (and semi-quantitative) effect of the main plasmon resonance is already contained in the 2D simulation.

VI. RETARDATION EFFECTS

So far, all the calculations have been performed within the electrostatics approximation. This is strictly speaking valid for very small objects $a \ll \lambda$, where the electric field can be assumed to be constant over the object. In practise, retardation effects can become non-negligible in the visible range for objects of dimensions ≈ 30 nm ($\lambda/10$). Retardation effects tend to red-shift the plasmon resonances and add more structure to the resonance profile. In order to appraise the effect of retardation on the depolarization ratios, we used Mie theory [22] to calculate exact results for the simple case of 3D spheres. We follow the treatment of Mie theory given by Bohren and Huffman [23]. For a sphere of radius a, we calculate the exact value of the field at the surface $\vec{E}(a,\theta,\phi)$. We can then evaluate the relevant integrals to calculate SERS intensities and depolarization ratios as before. In particular in the $Iso-B$ case, we calculate:

$$I_{\parallel}^{Iso-B} = \int_S |E|^2 |E_z|^2 dS, \tag{46}$$

$$I_{\perp}^{Iso-B} = \int_S |E|^2 |E_y|^2 dS, \tag{47}$$

$$I_{\perp 2}^{Iso-B} = \int_S |E|^2 |E_x|^2 dS. \tag{48}$$

$I_{\perp 2}$ is a magnitude that cannot be measured when detecting along the excitation direction x, but will be useful nevertheless to calculate other ratios. The depolarization ratio is then

$$\rho^{Iso-B} = \frac{I_{\perp}^{Iso-B}}{I_{\parallel}^{Iso-B}}. \tag{49}$$

By considering molecules of random orientations, one can also show that:

$$I_{\parallel}^{Rand-B} = \frac{2}{15}\left[3I_{\parallel}^{Iso-B} + I_{\perp}^{Iso-B} + I_{\perp 2}^{Iso-B}\right], \tag{50}$$

$$I_{\perp}^{Rand-B} = \frac{2}{15}\left[I_{\parallel}^{Iso-B} + 3I_{\perp}^{Iso-B} + I_{\perp 2}^{Iso-B}\right], \tag{51}$$

$$\tag{52}$$

and

$$I_{\parallel}^{Rand-C} = \frac{2}{35}\left[5I_{\parallel}^{Iso-B} + I_{\perp}^{Iso-B} + I_{\perp 2}^{Iso-B}\right], \tag{53}$$

$$I_{\perp}^{Rand-C} = \frac{2}{35}\left[I_{\parallel}^{Iso-B} + 5I_{\perp}^{Iso-B} + I_{\perp 2}^{Iso-B}\right]. \tag{54}$$

$$\tag{55}$$

The corresponding depolarization ratios ρ^{Rand-B} and ρ^{Rand-C} can then be evaluated.

In Fig. 5 we display the results for the $Iso-B$ case, for sphere radii in the range $a = 1$ to $a = 60$ nm. As expected, the results for $a = 1$ nm are identical to those obtained from the electrostatics approximation. As a increases, retardation effects lead to a number of modifications: First the plasmon resonance is split into several resonances, one of which red-shifts more the larger the radius. The maximum SERS intensity also decreases as a increases. Concerning the depolarization ratios, the most interesting point is that it shows virtually no change beyond its original resonance at 368 nm. In particular, the most red-shifted resonances of the intensity (which are the ones most relevant to SERS) do not affect ρ. Instead, ρ is modified in the regions of the secondary resonances. A closer look at the data indicates that ρ shows a dip for each of the resonances in the intensity (except the most red-shifted one). For example, for $a = 30$ nm, two dips at 358 and 374 nm are observed for ρ, and they correspond to peaks in the intensity profile. However, the most red-shifted resonance (at $\sim$432 nm) does not affect the profile of ρ. We conclude that in the regions of interest to SERS, retardation effects do not in general affect the main conclusions on depolarization ratios gained from the simpler electrostatic approach.

VII. COUPLED RESONANCES - CASE OF A DIMER

Finally, it is widely believed that the largest SERS enhancements originate from interactions between two or more particles, leading to coupled plasmon resonances. In many situations, it is likely that the SERS signal originates mainly from such interactions. We would therefore like to enquire whether such coupled resonances could affect our conclusions on the depolarization ratios. To do so, we calculated the depolarization ratio in the electrostatics approximation for two closely spaced 2D disks separated by $d = 0.1a$ (where a is the radius). The results are summarized in Fig. 6. The structure of the SERS intensity profile in the region of the single plasmon resonance (from 300 to 380 nm) is very complex. The coupled plasmon resonance is substantially red-shifted to 440 nm in this case (404 nm for a separation of $d = 0.2a$, not shown). This resonance is also the one exhibiting the highest integrated SERS intensity, as expected. The complexity of the intensity profile is due to the averaging of all possible orientations. In the literature, no orientation averaging is usually considered, hence the intensity

profiles exhibit much less structure in general. A wide variety of depolarization ratios is observed depending of the assumption made. Some of the discarded models in this section (like $Tan-A$, $Tan-B$, and $Tan-C$) predict values for ρ well above 1, a situation not observed experimentally. The most surprising result of the inclusion of coupled plasmons in dimers is that they seem to affect only the SERS intensity but not so much ρ, as can be observed in Fig. 6. When compared to the results for a single disk (see Fig. 7 for example), coupled resonances appear to narrow the resonance profile of ρ and make it tend faster towards its limiting long wavelength value. This leads to a small decrease in ρ for intermediate wavelengths.

Some of the other models not shown in the figure like $Norm-B$ and $Norm-C$, show a ρ that tends quickly towards its limiting value of $1/5$, which was also predicted for disks and spheres (2D and 3D) and ellipses (2D). A value of $\rho = 1/5$ should therefore be observed in most SERS conditions if one of these assumptions were correct. This is not the case, for experiments with a particular analyte like BTZ2 (used in the experimental section later on), but could be correct in other cases. We therefore conclude that the assumptions $Norm-B$, and $Norm-C$ for the interaction of the dye with the metal cannot apply for the specific analyte we shall explore later.

VIII. SOME EXPERIMENTAL EVIDENCE

We have already ruled out a number of possibilities and now concentrate on the most likely ones in terms of a possible connection with experimental results, namely: $Iso-B$, $Rand-B$ and $Rand-C$ models. All three cases show a qualitatively similar behavior, which is summarized in Fig. 7 for the case $Rand-C$ for various model geometries. We can draw from the previous calculations a number of conclusions about the depolarization ratios in these cases:

- In a SERS experiment on colloidal solutions with non-interacting colloids, where single colloids would contribute to a substantial fraction of the intensity, one should in principle observe signals from a distribution of spheroidal colloids, and possibly some elongated ones. One therefore expects to observe a ρ of a maximum of about 0.7-0.9. However, we saw in two instances (2D ellipses, and 3D spheres with retardation), that the maxima of ρ corresponded to dips in the SERS intensity, and vice-versa. If the excitation wavelength λ_L is within the range of particle resonances, resonant particles will contribute more to the signal, and a smaller value for ρ should be observed (we are in the dip associated with a maximum of SERS intensity). When λ_L is increased beyond most particles resonances, ρ should go through a maximum and eventually decrease slowly towards a limiting value depending on the model chosen. However, this limiting value is very difficult to measure, because the SERS intensity also decreases substantially.

- In interacting colloid solutions, SERS signals coming from interacting colloids will overwhelm that coming from single particles. Since the predicted depolarization ratio of a dimer vary little with wavelength at the coupled red-shifted resonance and beyond, one would expect a constant ρ at long wavelengths. ρ should also increase as λ_L is decreased towards the single (uncoupled) plasmon resonance. Other scenarios could be considered: for example, because the signal comes from a collection of various interacting objects, some interactions may be more dominant at some wavelengths. In a simple dimer picture, one expects that as the wavelength increases, more coupled (and therefore more red-shifted) resonances are dominating the signal. A calculation of 2D dimers with different separations shows that increased coupling should have a negligible effect on ρ. Another possibility is that the colloids may be able to merge and form a single elongated particle. Their behavior could then be more similar to that of an ellipsoidal particle.

Far from attempting a full experimental study of the effects reported here for reasons of space, we give an experimental indication of some of the important aspects that can be observed experimentally which do support the idea that depolarization ratios in SERS are affected by plasmon resonances. Accordingly, we measured depolarization ratios of SERS active liquids under various conditions and at different wavelengths.

The experimental details are identical to those reported in Ref. [24], except for the analyte which in these experiments is the newly developed benzotriazole dye: 4-(5'-azobenzotriazolyl)naphthalen-1-ylamine (BTZ2)[26]. The samples were prepared by mixing 0.5 mL of silver colloids[25] with 0.5 mL of water or KCl (concentration 10 mM), and adding 40 μL of 5 μM BTZ2 to obtain an end concentration of 0.2 μM of dye. The samples were then diluted by a factor of 4 (in water or KCl) to test for a possible effect of with multiple scattering on the depolarization ratio. No evidence for this were found when comparing diluted and non-diluted samples. To calculate depolarization ratios, the signals were averaged over periods between 5 and 20 minutes, to avoid problems associated with SERS fluctuations. The ratios is then estimated for 3 consecutive experiments to check for reproducibility and estimate errors.

These samples are stable for several weeks at room temperature. There is substantial experimental evidence of poly-dispersion in such Ag colloidal solution. Figure 8 gives a more definite idea of the complexity of real colloids, like the ones we used in the experiments reported below, in terms of size and/or shape distribution. The colloids have an average radius of $a = 30$ nm and exhibit

an absorption spectrum peaking at 454 nm. Spheres of $a = 30$ nm should have a resonance at 430 nm, and the observed red-shift in absorption is therefore attributed to variations in the shape of the particles. Without KCl, there is a strong coulombic repulsion among particles, and the SERS signal originates from single particle resonances. The addition of KCl results in a screening of this repulsive force, making the occurrence of closely spaced pairs more likely either by collisions or direct formation of dimers or small clusters. This is enough to observe a large increase in SERS signal, which shows that interacting particles dominate the signal. Such samples remain however stable with no aggregation into large clusters.

BTZ2 has several Raman peaks, the most prominent being around 1410 cm^{-1}. We measured the depolarization of this peak for a high dye concentration in water (no colloid) with 514 nm excitation and obtained $\rho = 0.33$, indicating a uniaxial Raman tensor. The depolarization ratios for this peak measured under SERS conditions are summarized in Fig. 9 as a function of laser wavelength, for samples without KCl (single particles) and with KCl (interacting particles). It is interesting to note that under SERS conditions, the depolarization ratios of all the other peaks was nearly the same as this one; a situation not happening in the pure dye and confirming that ρ is mainly determined by plasmon resonances rather than by the Raman tensor of the peaks. The background (or continuum, a well-known characteristic of SERS) also exhibits the same depolarization ratio, indicating its origin is strongly related to that of the SERS signal. Our experimental findings are consistent with the previous discussion for this specific experimental implementation. The models $Rand - C$, $Rand - B$, or $Iso - B$ show a good qualitative agreement. $Rand - C$ shows the best quantitative agreement, while $Rand - B$ seem to be predict too high a depolarization ratio at longer wavelength. $Iso - B$ is not relevant to this specific experiments, since we know from the depolarization ratio measurement in the pure dye that the tensor is not isotropic, at least when not adsorbed on the metal. Note the clear presence in Fig. 9 of a dependence on both the laser excitation and the KCl concentration, which reveals the role of plasmon resonances brought about by interactions among colloids. Both effects are expected from the general considerations presented in this paper. We discuss briefly the results in the next section.

We believe that further experiments on depolarization ratios could prove useful to the general understanding of SERS. In particular, experiments where parallel and perpendicular polarization intensities can be monitored simultaneously would enable one to study the fluctuations of ρ with time. This could provide insight into the origin of the SERS fluctuations, and a test of their interpretation as coming from single molecules.

IX. DISCUSSION AND CONCLUSIONS

The rotationally invariant components of the Raman tensor measured by depolarization ratios have a limited amount of information about the symmetry of the vibration. If a new molecule is measured in liquid, of which no previous information is known, we can infer the symmetry of the Raman tensor only to a certain extent. In general a combination of techniques are required. The same limitations occur for the changes in depolarization ratios by the presence of plasmon resonances: there is only a limited amount of information we can infer about the orientation of the molecule on the surface and it is very likely that we cannot decide between two competing models in certain cases. Like in the original case without plasmons, a combination of techniques will be needed for that task.

Still, what this paper has unequivocally shown is that *plasmon resonances produce "anomalous" depolarization ratios in standard SERS conditions and that the presence of the plasmons cannot be neglected or ignored.* The key issue highlighted in this paper can be summarized with the textbook example of local fields presented in Fig. 2. SERS is about local fields, and the polarization of the local field does not follow directly from that of the incident field. In that respect, we can safely say that plasmons are the most important factors controlling the depolarization of the scattering process under SERS conditions and are responsible for the large number of anomalies seen in experiments; a large fraction of which have not been explained or remain unaccounted for. The experimental results of the previous section do suggest that both the excitation wavelength and the state of aggregation of the colloids (producing coupled plasmon resonances) play a role in the depolarization ratios that are observed experimentally.

In this respect, we also believe that the interpretation of depolarization ratios put forward in several previous publications[18, 19] will probably have to be revised. Depolarization ratios have been used in the past to infer something about the orientation of the Raman tensor of a few (or one) molecules, completely ignoring the fact that the laser and Stokes field couple to the local field through the local plasmons and their symmetries. We believe that a re-interpretation of the data including the role of the plasmons might be necessary in those cases.

Finally, the limited amount of experimental information we have at the moment seems to to favor model C with respect to B for the scattering efficiency. This is a longstanding unresolved issue in SERS: whether the enhancement operates separately for the laser and Stokes-field thus producing a factor of $\propto \left|\vec{E}\right|^4$ in the scattering efficiency, or whether it is only the enhancement at the laser frequency $\propto \left|\vec{E}\right|^2$ followed by a re-emission process. Far from resolving this issue here, we suggest that depolarization ratios could help to discard possibilities and

learn a bit more about the SERS mechanism at a microscopic level. This is a unique aspect of SERS provided by the fact that the probe is in direct contact with the local field.

X. ACKNOWLEDGEMENTS

PGE acknowledges partial support for this work by the Engineering and Physical Sciences Research Council (EPSRC) of the UK under grant GR/T06124. Discussions on SERS with M. Cardona (Max-Planck-Institute, Stuttgart), Lesley Cohen (Imperial College), and Robert Maher (Imperial College) are gratefully acknowledged. We are indebted to Richard Tilley and David Flynn (Victoria University) for help and advice with electron microscopy and to Mike Dalley for help with the SERS measurements.

[1] W. Hayes and R. Loudon, *Scattering of Light by Crystals* (John Wiley & Sons, New York, 1978), p. 112.
[2] D. A. Long, *Raman Spectroscopy* (McGraw, Ney York, 1977).)
[3] S. P. S. Porto, J. Opt. Soc. Am. **56**, 1585 (1966).
[4] J. G. Skinner and W. G. Nielsen, J. Opt. Soc. Am. **58**, 113 (1968).
[5] M. Moskovits, Rev. Mod. Phys. **57**, 783 (1985).
[6] A. Otto, in *Light Scattering in Solids*, edited by M. Cardona and G. Güntherodt (Springer, Berlin, 1984), p. 289.
[7] A. K. Sarychev and V. M. Shalaev, Phys. Reports **335**, 275 (2000).
[8] V. M. Shalaev, Phys. Reports **272**, 61 (1996).
[9] E. C. Le Ru and P. G. Etchegoin, Chem. Phys. Lett. **396**, 393 (2004).
[10] D. P. Tsai, J. Kovacs, Z. Wang, M. Moskovits, V. M. Shalaev, J. S. Suh, and R. Botet, Phys. Rev. Lett. **72**, 4149 (1994).
[11] P. Zhang, T. L. Haslett, C. Douketis, and M. Moskovits, Phys. Rev. B **57**, 15513 (1998).
[12] P. Etchegoin, L. F. Cohen, H. Hartigan, R. J. C. Brown, M. J. T. Milton, and J. C. Gallop, J. Chem. Phys. **119**, 5281 (2003).
[13] H. Xu and M. Käll, Phys. Rev. Lett. **89**, 246802 (2002).
[14] N. Calander and M. Willander, Phys. Rev. Lett. **89**, 143603 (2002).
[15] K. Kneipp, H. Kneipp, I. Itzkan, R. R. Dasari, and M. S. Feld, J. Phys: Condens. Matter **14**, R597 (2002).
[16] K. Kneipp, Y. Wang, H. Kneipp, et al., Phys. Rev. Lett. **76**, 2444 (1996).
[17] S. Nie and S. R. Emory, Science **275**, 1102 (1997).
[18] K. A. Bosnick, J. Jiang, and L. E. Brus, J. Phys. Chem. **106**, 8096 (2002).
[19] A. M. Michaels, M. Nirmal, and L. E. Brus, J. Am. Chem. Soc. **121**, 9932 (1999).
[20] All simulations in this paper where produced with Matlab [The MathWorks Inc. (www.mathworks.com)] with adaptive-mesh scripts for electromagnetic calculations generated by FEMLAB [Comsol Inc. (www.femlab.com)].
[21] *Handbook of Optical Constants of Solids, III*, edited by E.D. Palik (Academic Press, New York, 1998).
[22] G. Mie, Ann. Phys. **25**, 377 (1908).
[23] C. F. Bohren and D. R. Huffman, *Absorption and Scattering of Light by Small Particles* (Wiley, New York, 1983).
[24] R. C. Maher, M. Dalley, E. C. Le Ru, L. F. Cohen, P. G. Etchegoin, H. Hartigan, R. J. C. Brown, and M. J. T. Milton, J. Chem. Phys.**121**, 8901 (2004).
[25] P.C. Lee, D. Meisel, J. Phys. Chem. **86**, 3391 (1982).
[26] D. Graham, C. McLaughlin, G. McAnally, J. C. Jones, P. C. White and W. E. Smith, Chem. Commun. 1187-1188 (1998).

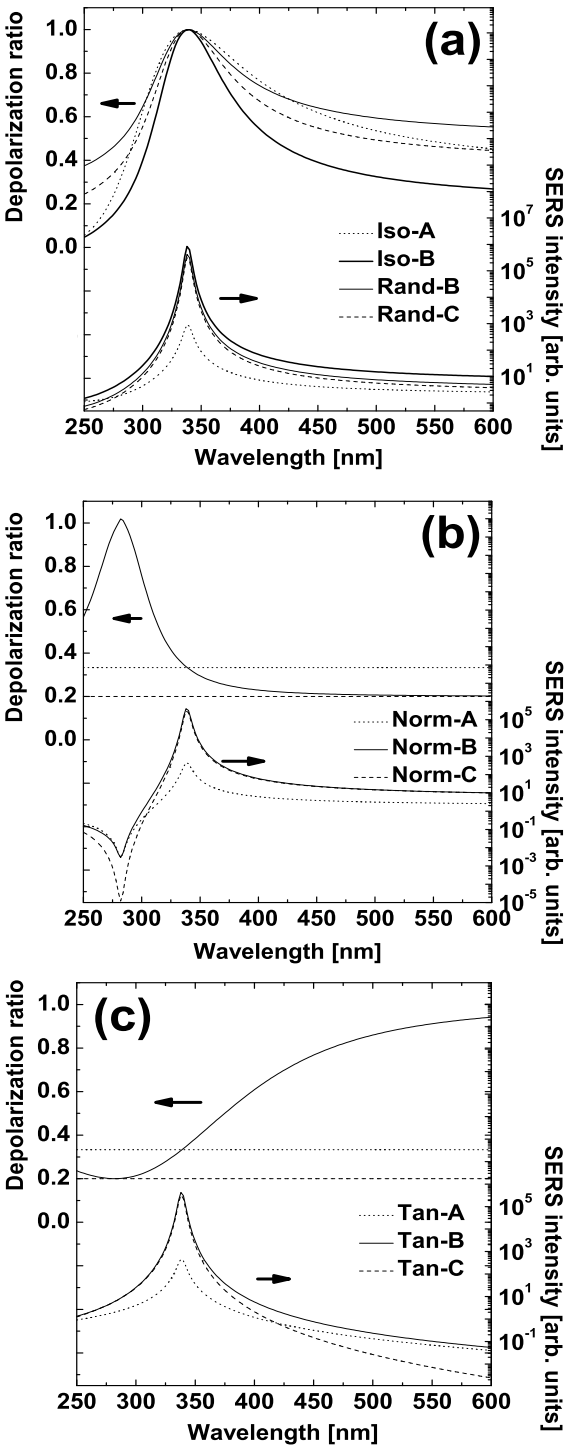

FIG. 1: Depolarization ratios and total SERS intensities calculated for a 2D disk from different assumptions as a function of wavelength. *Tan*, *Norm*, *Iso* and *Rand* define the type of Raman tensor under consideration, as specified in the text (Sec. II), while A, B, and C account for the different models of the scattering process defined in Eqs. (1), (2), and (3). Note that the SERS enhancements are plotted on a log-scale.

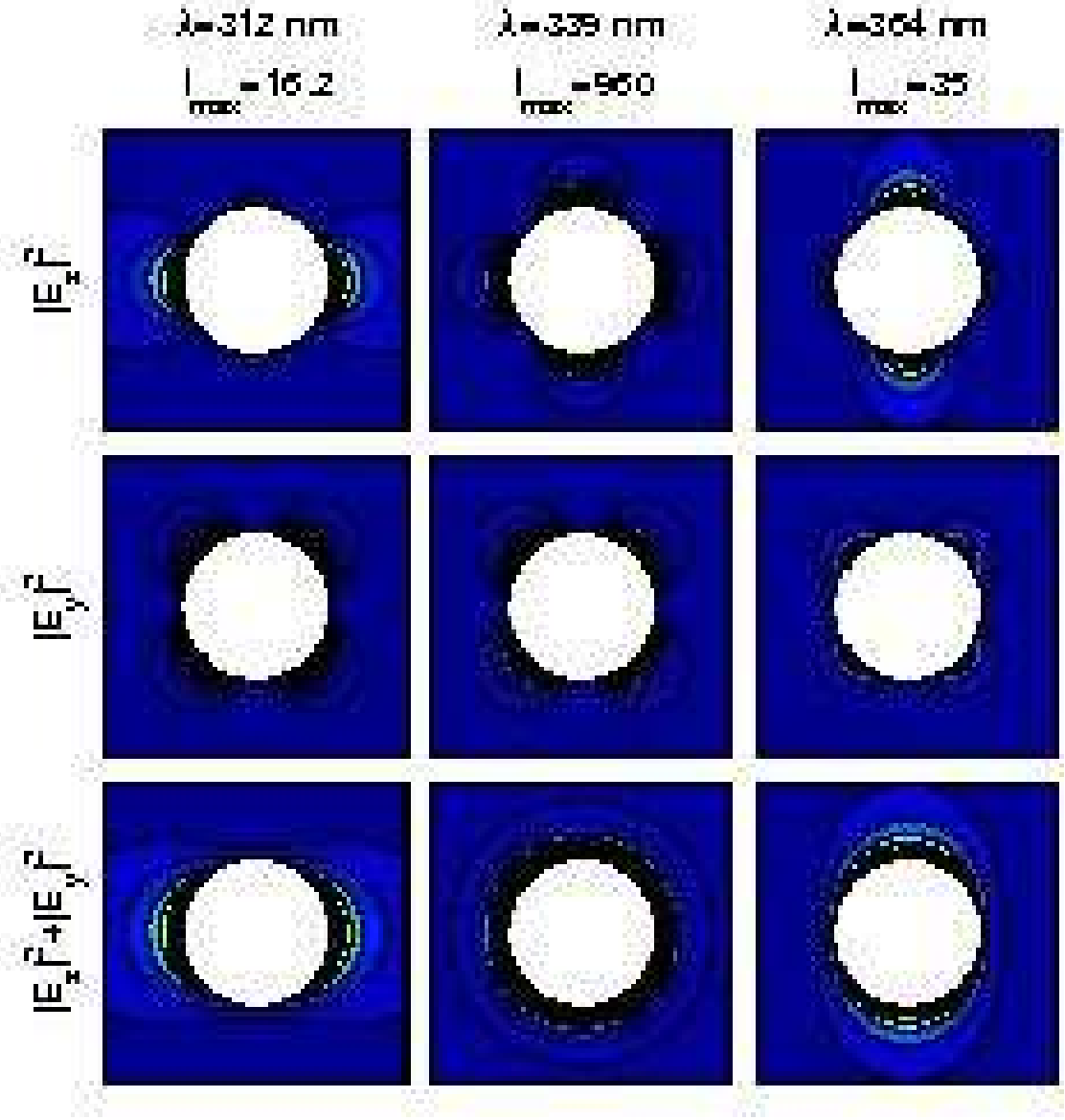

FIG. 2: Intensity patterns in a 2D disk at three different wavelengths (columns) for the field component along z (first row), y (second row), and for the total intensity (third row). The excitation polarization of the external field is along z. For a scatterer with an isotropic Raman tensor, for example, the integrated intensity on the surface of the disk for $|E_y|^2$ divided by that for $|E_z|^2$ defines the depolarization ratio ρ. By visual inspection, it is evident that the depolarization ratio will be smaller at 312 and 364 nm than at 339 nm, where the disk has its main resonance. Colors mean different intensities for the different columns; we provide the maximum field intensity for each wavelength at the top of each column. Red (blue) means high (low) intensity in a linear color scale. See the text for further details.

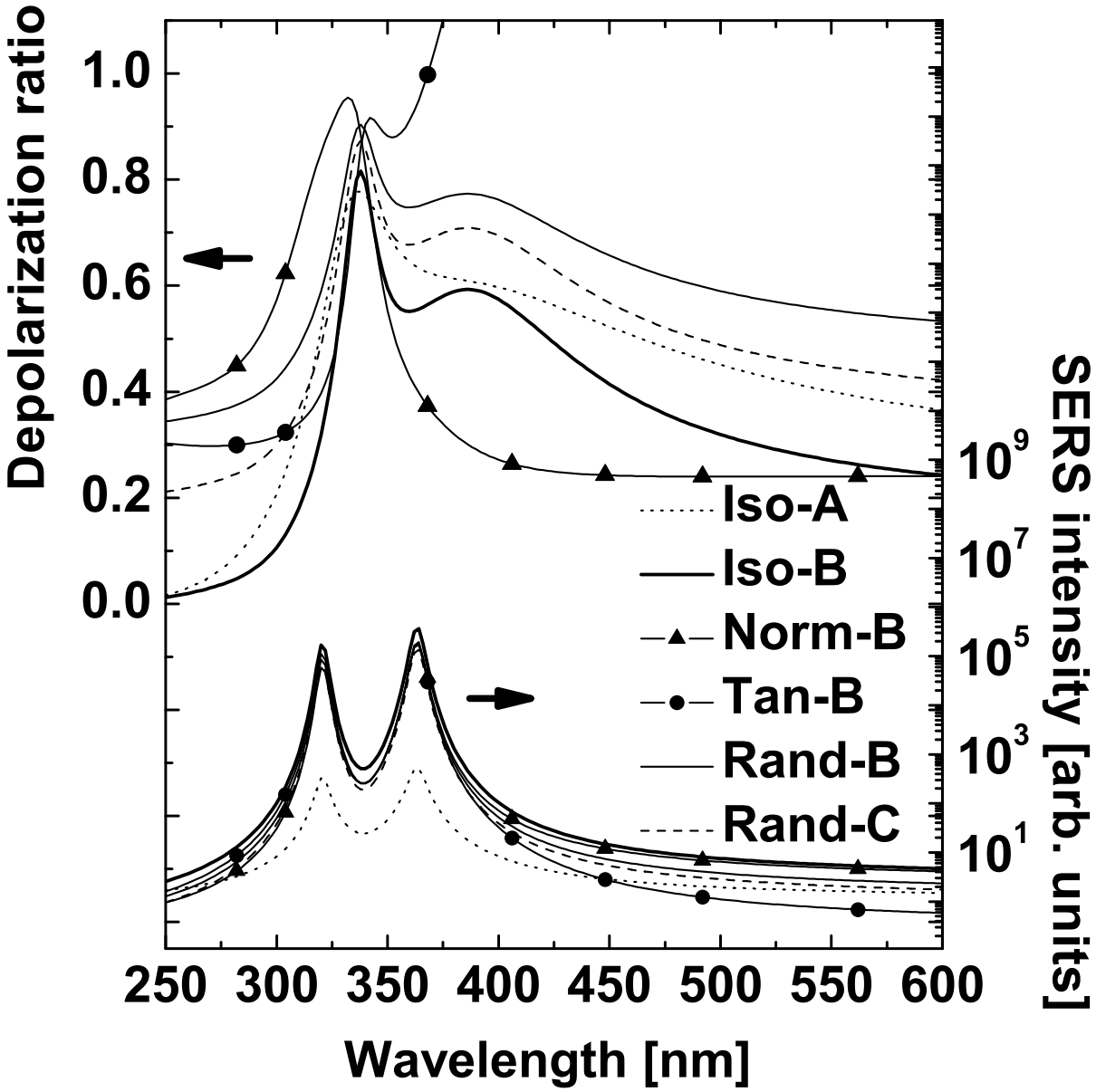

FIG. 3: Depolarization ratios (top) and total SERS intensities (bottom) as a function of wavelength calculated for an ellipse for some of the models presented in Fig. 1. As opposed to the case of a disk in Fig. 1, an ellipse has two main shape-related plasmon resonances in the SERS intensity profile. The $Tan-B$ model for the orientation of the molecule and the scattering mechanism gives depolarization ratios which go well above 1 across the visible range.

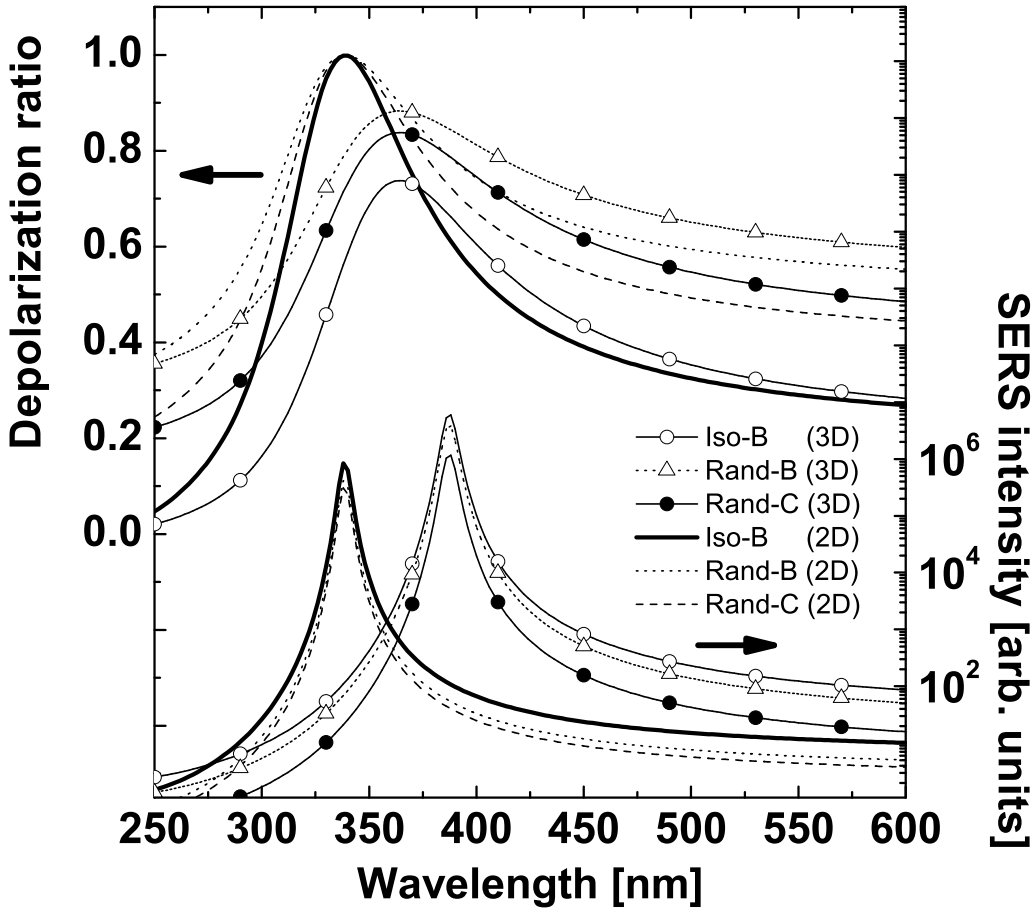

FIG. 4: Comparison between the depolarization ratios (top) and the total SERS intensities (bottom) calculated for a 3D sphere with those of a 2D disk. The curves with symbols (lines) are the 3D (2D) cases for models $Iso-B$, $Rand-B$, and $Rand-C$, respectively. The depolarization ratios together with the SERS intensities in this figure complete the qualitative/quantitative comparison of the effect of dimensionality on these quantities.

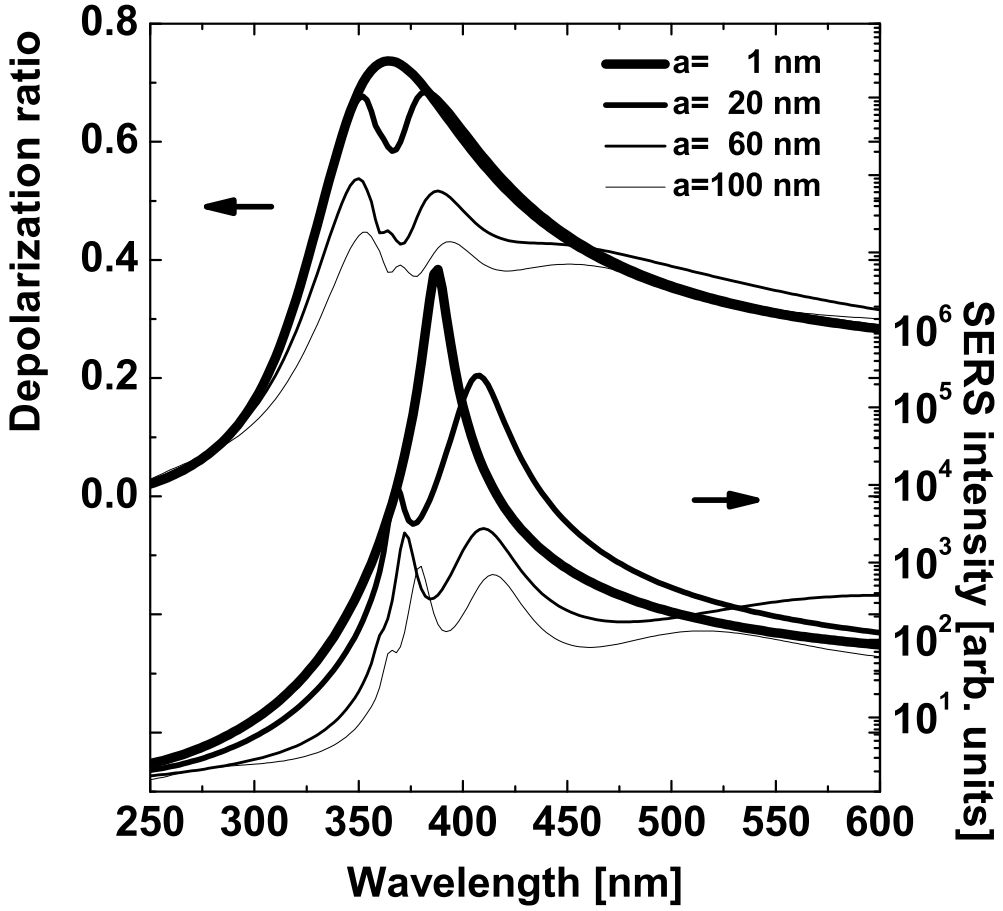

FIG. 5: Depolarization ratio (top) and SERS intensities (bottom) calculated using exact Mie theory for 3D spheres of various radii a from 1 to 60 nm. Thicker (thinner) lines represent smaller (larger) radii. The results are shown for the $Iso-B$ case.

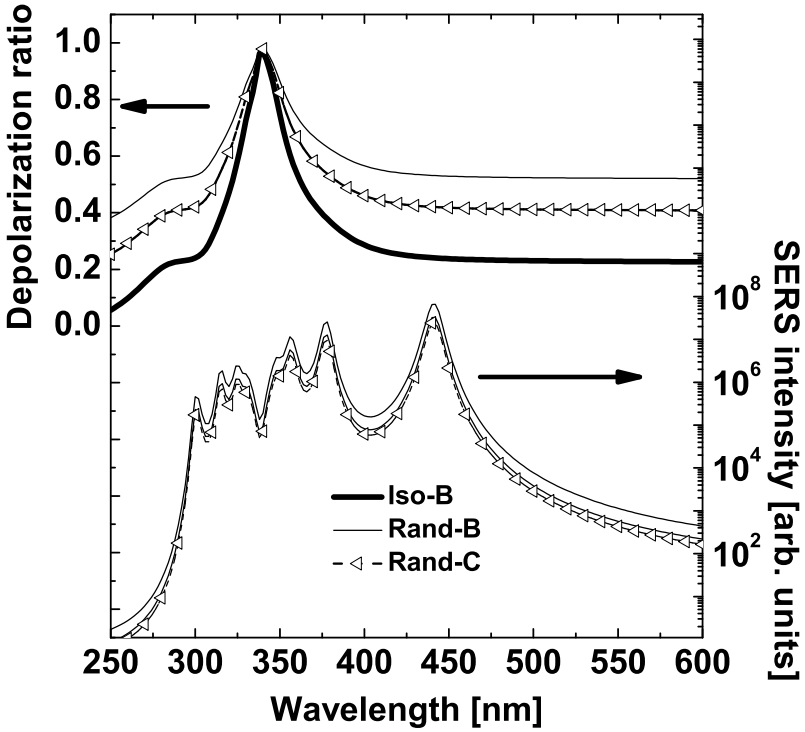

FIG. 6: Depolarization ratios (top) and SERS intensities (bottom) for $Iso-B$, $Rand-B$, and $Rand-C$, for a 2D dimer with separation $d = 0.1a$. Note that the depolarization ratio is not affected by all the structures appearing as resonances in the SERS enhancement.

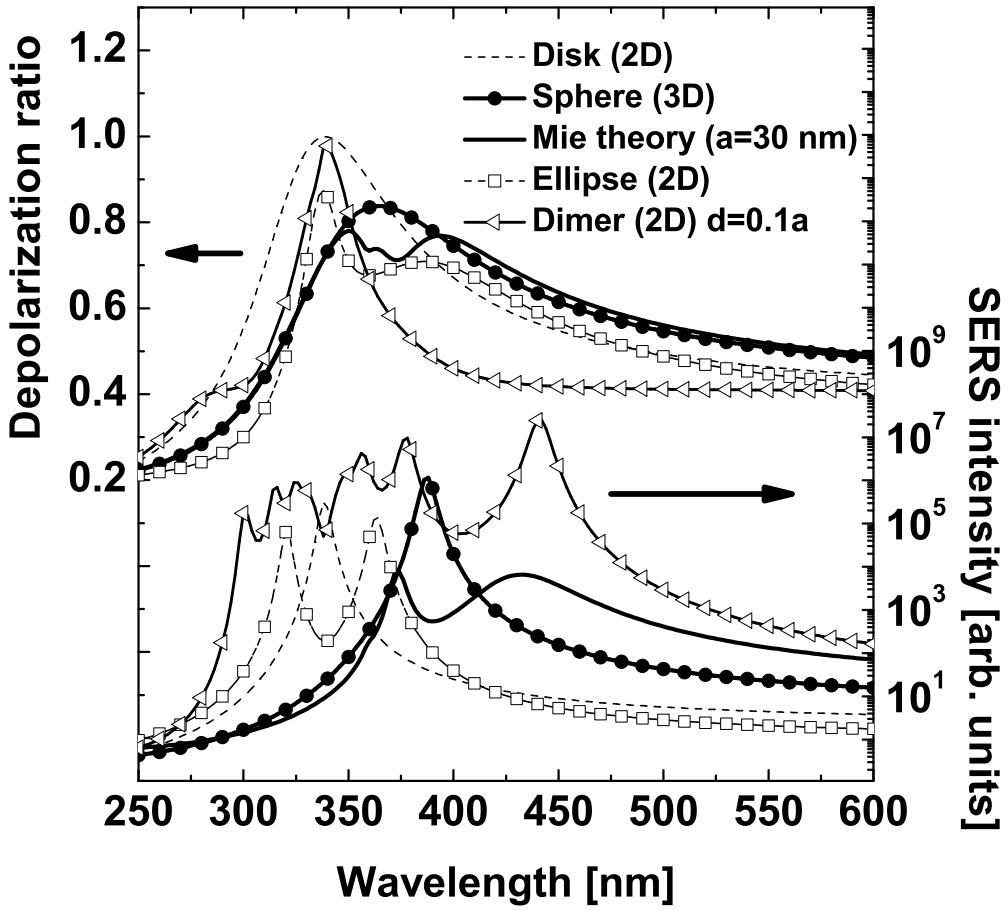

FIG. 7: Depolarization ratios ρ (top) and SERS intensities (bottom) for the case $Rand - C$ for different model geometries. This figure summarizes the various effects on ρ of shape, dimensionality, retardation, and coupled resonances.

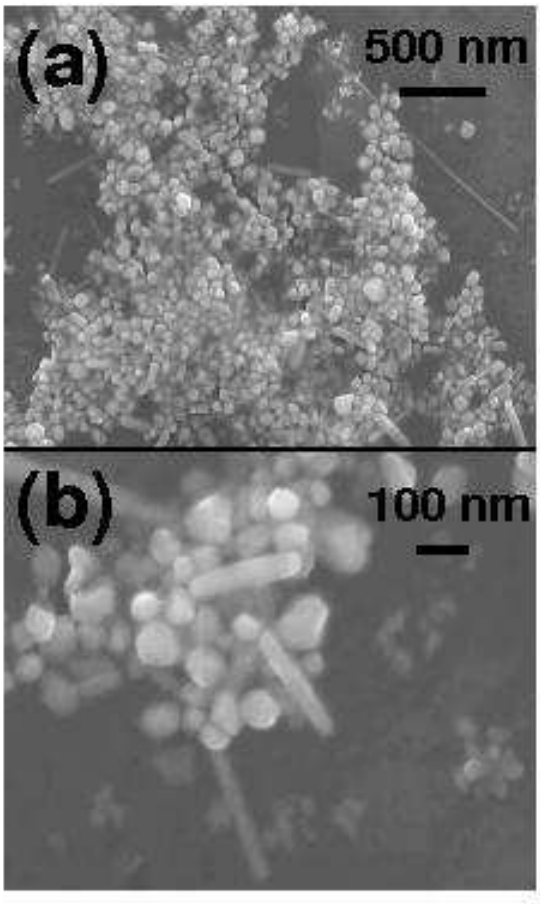

FIG. 8: Two scanning electron microscope images of Ag-colloids used in the experiments reported here and prepared by the method of Ref. [25]. The images are at different magnifications and give an idea of the typical spread in sizes (a) and the details of individual particles (b).

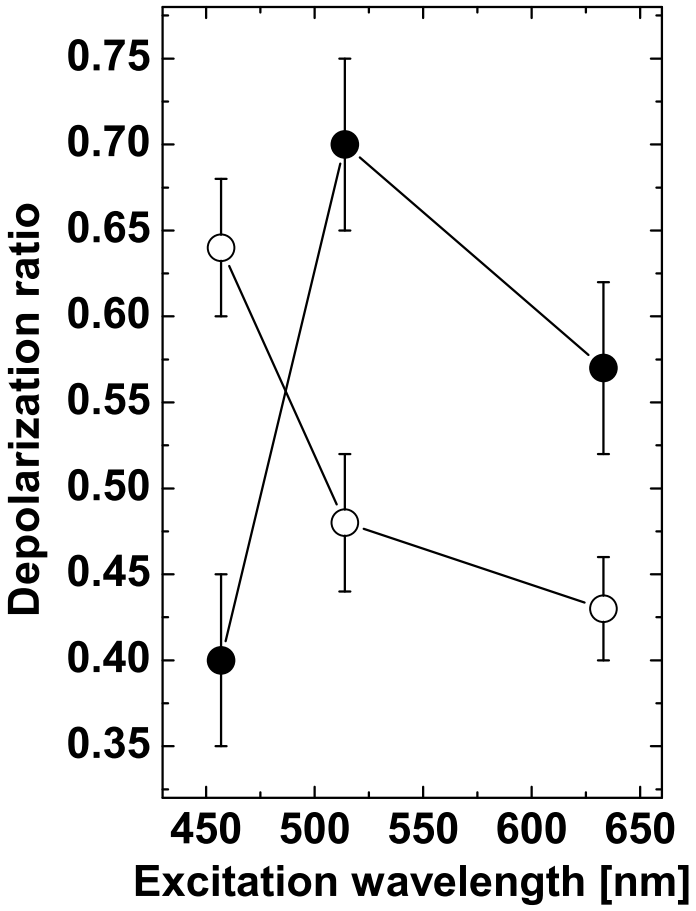

FIG. 9: Experimental depolarization ratios for 3 different laser excitations: 457, 514, and 633 nm, for a colloid sample with (empty circles) and without (solid circles) KCl. The analyte is the benzotriazole dye BTZ2. These data show a dispersion in laser wavelength as well as a change depending on the interacting state of the colloids (KCl concentration).